Construction and Building Materials 248 (2020) 118475

Contents lists available at ScienceDirect

Construction and Building Materials

journal homepage: www.elsevier.com/locate/conbuildmat

A novel support vector regression (SVR) model for the prediction of splice strength of the unconfined beam specimens

Mohammad Suhaib Ahmad [a], Sayed Mohammad Adnan [b], Sadaf Zaidi [c,*], Pradeep Bhargava [a]

[a] Department of Civil Engineering, Indian Institute of Technology Roorkee, Roorkee, UK, India
[b] Department of Chemical Engineering, Aligarh Muslim University, Aligarh, 202002 U.P., India
[c] Department of Post -Harvest Engineering and Technology, Aligarh Muslim University, Aligarh 202002, U.P., India

HIGHLIGHTS

- Three models based on M Non-linear Multi regression, (NMR), Artificial neural networks (ANN) and Support vector regression (SVR) are proposed.
- First time SVR is being used for the assessment of splice bond strength.
- Experimental data of 267 unconfined beam specimens were used including authors own experimental data.
- Proposed models show better performance in comparison to the existing models.
- SVR model shows great potential in the assessment of splice strength of unconfined beam specimens.

ARTICLE INFO

Article history:
Received 14 November 2019
Received in revised form 9 February 2020
Accepted 14 February 2020
Available online 19 March 2020

Keywords:
Splice strength
Unconfined beam specimen
Support vector regression (SVR)
Artificial neural network (ANN)
Non-linear multi regression (NMR)

ABSTRACT

Splice strength in reinforced concrete is an important parameter for the safe design of any structure which should be assessed with ease and accuracy. Analytically the assessment of splice strength is a complex problem because of the improper idealization of the stress field around the splice region. Further, for the empirical models, the assessment is still complicated due to the variable nature of materials used i.e. concrete and steel especially in case of high strength concrete beams. The focus of the study is to develop a robust model for the prediction of splice strength encompassing significant parameters in a wide range using support vector regression which is for the first time used for this assessment. Further, for the purpose of comparison, in addition to existing empirical models NMR (Nonlinear Multi-regression), and ANN (Artificial Neural Networks) models were also formulated. A data set of 267 splice beam specimens from the literature was used including the authors own generated data for the training and testing of the models. The parameters under consideration are the diameter of the bar, the compressive strength of the concrete, development length and cover to the reinforcement. The statistical analysis of the models suggests that NMR is better than the existing empirical correlations however inferior than the SVR and ANN models for the prediction of splice strength. Furthermore, SVR and ANN show comparable accuracy in predicting the splice strength of unconfined beam specimens however, SVR is found to be more efficient than ANN. The study concluded that SVR has the potential to predict the splice strength with higher accuracy in comparison to the prescriptive empirical relationships and can be used for design purposes.

1. Introduction

Splicing of the reinforcement in the reinforced concrete structural system is indispensable and provided in almost every structural element. The easiest way to achieve splicing in structural elements is through overlapping the reinforcing bar. The splicing ensures continuity of the reinforcing bars and the economic utilization of the reinforcing steel inside the structural elements. The stress transfer from the concrete to reinforcing steel in the splice region occurs through the bond action. The maximum stress that can be transferred from the concrete to steel is often termed as splice strength or bond strength and depends on many factors that include extent of the overlap l_s, diameter of the bar d_b, bar deformation pattern (relative rib area R_r), minimum cover to the reinforcement C_{min} and the compressive strength of the concrete $f_c^{'}$. The splice strength increases with the increase in the overlap length l_s however this increase is not proportional to the overlap length [1]. The smaller size diameter shows higher bond strength in

* Corresponding author.
E-mail addresses: mahmad1@ce.iitr.ac.in (M.S. Ahmad), s.zaidi.ke@amu.ac.in (S. Zaidi).

https://doi.org/10.1016/j.conbuildmat.2020.118475
0950-0618/

Nomenclature

A_b	Area of the bar in mm^2
$AARE$	Average Absolute relative error %
b	Bias for the function
C_{min}	Minimum cover to the reinforcement in mm
C_{med}	Median value of the bar covers in mm
C_{max}	Maximum cover to the reinforcement in mm
d_b	Diameter of the bar in mm
$f_c^{'}$	Cylindrical compressive strength of concrete in MPa
f_s	Stress in steel in MPa as per ACI – 408R
$f(x)$	Regression function
f_{stm}	Stress in steel in MPa as per FIB model code 2010
$g(x)$	Function describing high dimensional featured space
$K(x_i, x_j)$	Kernal function
l_s	Splice length or overlapped length in mm
M	Constants used for the bond strength of bars as per Esfahani and Ranjan (1998a, 1998b)
U_c	Bond strength of splice beam specimen as per Orangun, Jeersa and Breen(1977).
w	Weights of the network
x_i	i^{th} input vector

Greek letters

ω	Weight vector
ξ,ξ^*	Slack variables
$\alpha_i\alpha_i^*$	Lagrangian Multipliers
σ	Width of RBF kernel
γ	Regularization Parameter
ε	Loss function
$\Psi(x)$	Activation function

comparison to bars with larger diameters [2,3]. The splice strength remains almost unchanged with the change in the deformation pattern (relative rib area R_r) in the case of unconfined beam specimens [4]. However, the splice strength increases with the increase in relative rib area R_r in cases of confined splice beam specimens [5,6]. The confinement provided from the cover alone C_{min} is the minimum of the effective side cover C_s and the bottom cover C_b [7]. The effective side cover C_s is the minimum of the (side cover and half of the distance between the splices). The increase in concrete cover not only increases the bond strength but is also responsible for the mode of failure [8,9]. The smaller concrete cover (up to 2.5 times the d_b) causes a splitting mode of failure while the larger cover (above 2.5 times the d_b) can result in a pull-out mode of failure. The compressive strength $f_c^{'}$is the most important parameter influencing the splice strength. The splice strength is proportional to $1/n^{th}$ power of the concrete compressive strength. Different studies have proposed the power n for different ranges of concrete. Earlier the number n equaled to 2 was believed to be best representing the contribution of $f_c^{'}$ to the splice strength up to the range of 55 MPa [10]. However, this power overestimates the contribution of compressive strength in case of higher strength concrete beams. Later an extensive experimental study [7] suggests that n equals to 4 can best represent the contribution of concrete to splice strength for both high strength and normal strength concrete.

Apart from the experimental studies carried out in the past to understand the effect of different parameters as mentioned above, efforts have been consistently made by various researchers to predict the splice strength of the beam specimen encompassing these parameters. The first-ever known effort to predict the bond strength of the overlapped splice beam specimen was done by Tefpers [11]. He idealized the bond problem to a thick-walled cylinder with internal pressure p. Initially, this idealization was only for the lone deformed bar which he later modified for the overlapped bars by assuming that in the contact splice, the bars are placed side by side so that the total pressure will be due the interference of the two equal pressures generated due to two bars. However, this prediction was found to be unconservative and could not be used for engineering purposes.

Later, Esfahani and Ranjan [12,13] modified the Tepfers [11] partly cracked cylinder theory for the prediction of bond/splice strength of unconfined normal and high strength concrete beam specimens. They established bond strength in terms of the tensile strength of the concrete and cover to diameter ratio of the bar C/d_b for both normal and high strength concrete. The relationship was established for short bond length using pull out specimens. Further, these semi-empirical relationships were used for the formulation of an analytical equation that can predict the splice / bond strength of the overlapped beam specimens. The equation proposed was as follows.

$$\frac{A_b f_s}{\sqrt{f_c'}} = 2.7\pi l_s \frac{(C_{min} + 0.5d_b)(1+\frac{1}{M})}{\left(\frac{C_{min}}{d_b} + 3.6\right)\left(1.85 + 0.024\sqrt{M}\right)} \left(0.12\frac{C_{med}}{C_{min}} + 0.88\right) \quad (1)$$

where $M = \cosh(0.0022 l_s \sqrt{r f_c'/d_b}$

Orangun, Jirsa and Breen [10] proposed an empirical equation based on multilinear regression analysis of 62 overlapped splice beam specimens as given by Eq. (2).

$$\frac{u_c}{\sqrt{f_c'}} = 0.10 + 0.25\frac{C_{min}}{d_b} + 4.15\frac{d_b}{l_s} \quad (2)$$

The parameters under consideration were overlapped length, cover to the bar, diameter of the bar and the concrete compressive strength.

Darwin et al. [14] introduced the effect of the ratio of relative cover thickness (C_{max}/C_{min}) and the relative rib area R_r on the splice strength of the beam specimen. Later the same authors Zuo and Darwin [5] increased the database of the beam specimens by including beams of high strength concrete and proposed an empirical relationship as given in Eq. (3) in which the contribution of the compressive strength was ¼ power in place of ½ which was earlier proposed. This departure in the power was because the power of ½ overestimates the contribution of compressive strength in the high strength concrete beams.

$$\frac{A_b f_s}{(f_c')^{1/4}} = (1.43 l_s(C_{min} + 0.5d_b) + 56.2A_b)\left(0.1\frac{C_{max}}{C_{min}} + 0.90\right) \quad (3)$$

Besides equations available in the literature, a separate code for the assessment of splice strength was also presented by ACI as ACI 408 R [15]. The code also suggests an empirical relationship which is actually the adaptation of the equation of Zuo and Darwin [5] with minor modifications as shown below

$$\frac{A_b f_s}{(f_c')^{1/4}} = (1.43 l_s(C_{min} + 0.5d_b) + 57.4A_b)\left(0.1\frac{C_{max}}{C_{min}} + 0.90\right) \quad (4)$$

The FIB modal code 2010 [16] also proposes a semi-empirical equation for the assessment of splice strength. The equation is non-linear in nature unlike ACI 408 R. The equation with the usual notations is shown below.

$$f_{stm} = 54\left(\frac{f_{cm}}{25}\right)^{0.25} \cdot \left(\frac{25}{d_b}\right)^{0.2} \left(\frac{l_s}{d_b}\right)^{0.55} \cdot \left(\frac{C_{min}}{d_b}\right)^{0.25} \cdot \left(\frac{C_{max}}{C_{min}}\right)^{0.1} \quad (5)$$

Recently machine learning (ML) has been employed by researchers in different areas of civil engineering out of which structural engineering found its relevance in health monitoring, mechanical properties of concrete, fracture mechanics, steel-concrete interface as well as post-fire mechanical properties of concrete and even in fire resistance of RC beams [17–23]. However, these applications are often based on traditional techniques like ANN which works on the principle of empirical risk minimization (ERM). SVR is another set of supervised ML technique which works on the principle of structural risk minimization (SRM). SVR can be applied for both classification as well as for regression. Lie et al. [24] applied SVM and neural networks on their experimentally generated data for the prediction of concrete compressive strength. The parameters under consideration were the amount of: cement, water, fine and coarse aggregate and silica fume. The authors concluded that both the techniques proved to be a great success in the prediction of compressive strength with the same accuracy. However, SVR was observed to be more efficient than ANN in terms of computational effort. In an attempt to explore the potential of SVM in the field of geotechnical engineering, Pijush Samui [25] successfully applied the SVM model in predicting the complex problem of support settlement of shallow foundations on cohesionless soil. Also, he performed a comparative study of SVR with other existing empirical and ANN models in which he observed that the SVR proved to be most effective and efficient. Yuvraj et al. [21] developed an SVR based model utilizing their experimental data for the estimation of the characteristic parameters describing fracture of high strength and ultra-high-strength concrete beams. The characteristic parameters included fracture energy, failure load, critical stress intensity factor and critical crack tip opening displacement. The independent variables considered in this study were cross-sectional area, depth of the notch, water to cementitious material, length of the specimen and strength of the concrete. The model was observed to be in good agreement with the experimental data.

1.1. Research significance

The above literature review shows that the existing theoretical models (based on thick wall cylinder theory) overestimate the splice strength of the beam specimens because of the complex interaction between deformed reinforcing bars and concrete in the spliced region. Further, the empirical equations proposed are based on multilinear regression analysis due to which effect of individual parameters on the bond strength cannot be understood. Realizing the complexity of the problem in idealizing the splice bond strength and a requirement of better methodology which can predict the splice bond strength with ease and express the effect of individual parameters on the bond strength is the need of the hour. Further, the literature also suggests that machine learning techniques especially SVR have shown great potential in solving complex engineering problems accurately and efficiently without actually getting involved in the mechanics of the problem.

Hence, it was planned to develop a model based on support vector regression which can accurately estimate the splice strength of unconfined beam specimens. The above-stated objective was achieved by training the SVR model on existing data from literature and later testing the model on the data which includes the authors' experimentally generated data. For the purpose of comparison, the existing empirical models and codes which include ACI 408-R and FIB model code 2010 have been used. In addition, two new models were also developed based on nonlinear multi regression (NMR) and artificial neural networks (ANN). The performance of the SVR based model was determined by comparing the values of its statistical performance indicators like AARE, RSME, MRE and QLOO with those of the existing models as well as the NMR and ANN models developed in the present study.

2. Experimental program

The experimental program consisted of casting, curing and testing of eight splice beam specimens of normal strength concrete. The parameters under consideration were the diameter of the bar (12 and 20 mm), development length (120 and 200) mm, and cover to the bar (20 and 40 mm).

2.1. Test specimens

The beam specimens were 1300 mm long with a constant overall depth of 230 mm and a varying width ranges from 150 to 230 mm. The bars in the bottom were spliced in the middle to the beam specimen. To avoid complexity in the analysis equal nominal covers were provided to the reinforcement at the bottom and at both sides of the beam. Further, for the shear strengthening, single-legged 8 mm stirrups were provided at a spacing of 70 mm in the varying moment zone. This restriction ensured that the bond behavior observed during testing was only due to the effect of concrete. Also, the beam specimens were provided with slots in the bottom in the constant moment zone. This type of design enabled us to install the required instrumentation during the mechanical loading of the beam specimen to capture strains in the reinforcing bars during testing. The full details are shown in Fig. 1.

2.2. Materials

The concrete mix was achieved using Ordinary Portland Cement of grade 43 conforming to IS 8112-1989 [26]. The locally available crushed limestone was used as coarse aggregate with the maximum size of 12.5 mm conforming to IS grade [27] while the naturally available river sand was used as fine aggregate. The details of the mix proportioning are shown in Table 1.

Commercially available high grade ribbed reinforcing steel bars of yield strength 500 MPa were used as flexural and shear reinforcements. The mechanical and surface bar properties of the bars used in the investigation are given in Table 2.

2.3. Casting and curing details

The beam specimens were cast in the vertical position in steel moulds so that the reinforcing steel was in the bottom position during casting. The position during casting is important since it can affect the bond strength of the beam specimens. All the eight specimens were cast continuously in three batches of the concrete. Representative concrete cylinders and cubes were also cast each time a mix is prepared. The specimens were cured for a duration of 28 days using wet hessian cloth and were kept in a controlled environment of temperature 25 °C and relative humidity of 92% till the testing. A length of half the depth of the beam specimens was de-bonded from the splice ends on either side for the purpose of instrumentation before the beams were finally taken for the mechanical loading.

2.4. Testing procedure and instrumentation

The beams were mechanically tested under four-point bending in a closed-loop servo-controlled HICO flexure testing machine of 350 kN capacity. The symmetrical loading arrangement ensured constant moment region in the spliced zone. The distance between the applied loads was kept equal to the sum of splice length and

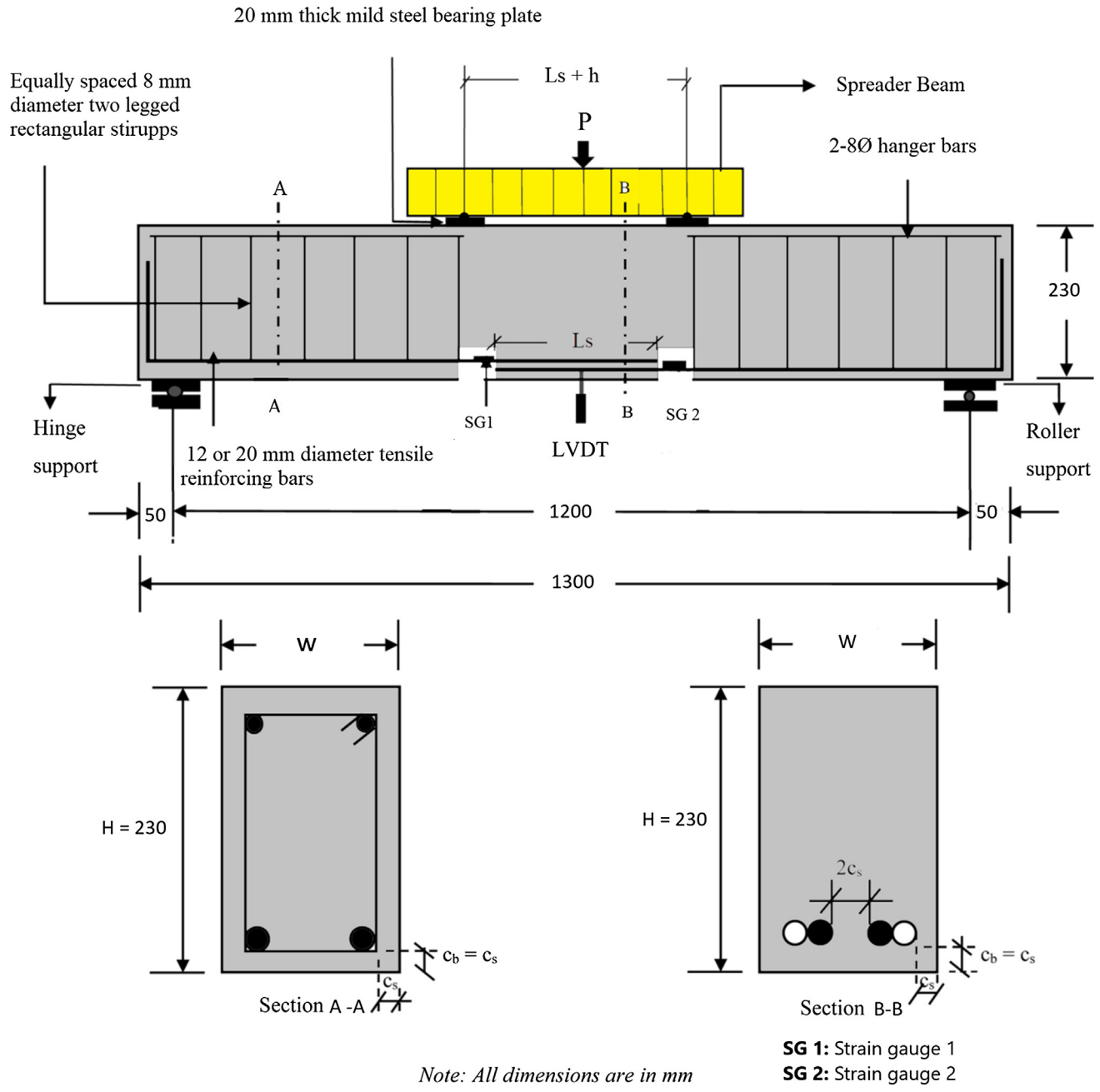

Fig. 1. Geometrical details and the loading arrangement of the beam specimens.

Table 1
Mix proportion of the concrete.

Cement (kg)	Coarse Aggregate (kg)	Fine Aggregate (kg)	Water Content (kg)	Super Plasticizer (kg)	W/C ratio
400	825	1004	168	0.002	0.44

Table 2
Mechanical and bar surface properties.

Bar diameter (mm)	Yield strength (MPa)	Ultimate strength (MPa)	Elongation (%)	Rib height h_r (mm)	Rib spacing S_r (mm)	Relative rib area (h_r/S_r)	Rib face angle α°
12	571.61	662.58	12.5	0.70	7.28	0.096	45
20	560.85	656.2	17.55	1.03	10.89	1.095	41

the beam depth. The specimens were loaded under displacement control mode at a constant rate of 0.005 mm/s. Vertical and horizontal cracks were monitored constantly during the whole experimentation. For the purpose of obtaining the strains in steel during the mechanical loading, strain gauges were installed on the un-bonded region of the spliced reinforcing bars. Further, for the measurement of mid-span deflection, LVDT was installed under the beam specimens at mid-span. The details are shown in Figure 1.

2.5. Stress in steel

The obtained strains at failure were converted to stresses by multiplying them to the elastic modulus. The stresses in the reinforcing steel for all the beam specimens are reported in Table 3. The reported stress for each beam was the average stress from the two reinforcing bars observed during the experimentation. The stress in steel was reported instead of bond strength because in practice the bond stress varies along the length of the splice [28] and most of the empirical equations predict the stress in steel instead of bond strength. The stress in steel was also calculated using the moment-curvature relationship which confirmed that the values obtained from the strain gauges were consistent.

3. Data collection and pre-processing

In the current study, first of all the data generated by the authors in their experiments and that collected from the various sources [29–43] was tested for outliers. The data set was so chosen that it should cover all the data points that have been used by other researchers for the formulation of their empirical/theoretical models so that a fair and distinct comparison could be performed. Secondly, the significance of the parameters affecting the splice strength of unconfined beam specimens was tested. The significant parameters observed were diameter of the bar d_b, strength of the concrete $f_c^{'}$, cover to reinforcement both maximum and minimum, C_{max}, C_{min}, and splice length l_s The parameters under consideration and their ranges are shown in Table 4. For each of the three models, the entire data set consisting of 267 data points were first randomized and subsequently normalized before finally partitioned into two sets namely training and testing data. The training data set comprising 80% of the data and the test set containing the remaining 20% of the data. The random selection of data was to avoid any bias to the models. For all the three models, the training data set was used for model development and the test data set was used for testing the models.

4. Computing methodology

In this part of the paper different modeling techniques that are applied on the data to develop models for the estimation of splicestrength have been discussed. These include a statistical nonlinear regression model, and two machine learning-based models namely, SVR model and ANN model.

4.1. Nonlinear Multiregression (NMR) model

Non-linear regression is an attempt to establish a mathematical relationship between the dependent variables and the independent variables through a process of fitting. The independent variables are raised to different powers which represent their contribution towards the dependent variable. The relationship is generally formulated as a power-law equation as shown below:

$$\varnothing = a_0 \cdot Z_1^{a_1} \cdot Z_2^{a_2} \cdot Z_3^{a_3} \tag{6}$$

Later these parameters were utilized to idealize a nonlinear relationship with the output variable, splice strength which is in the form.

$$fs = a_o.(d_b)^{a_1}.(l_d)^{a_2}.\left(f_c^{'}\right)^{a_3}.(C_{min})^{a_4}.(C_{max})^{a_5} \tag{7}$$

where f_s is the stress in steel or the splice strength $a_1 \cdots\cdots a_5$ are the exponents of the independent variables and a_0 is a constant.

Further, the regression was performed on the training data set and the model was validated on the test data set

In order to perform the regression, Eq. (7) was linearly transformed by taking log on both sides as shown in Eq. (8).

$$log_{10}f_s = log_{10}a_0 + a_1.log_{10}d_b + a_2.log_{10}l_d + a_3.log_{10}C_{min} + a_4.log_{10}C_{max} + a_5.log_{10}f_c \tag{8}$$

The Regression finally yields the value of the constant a_0 and the coefficients $a_1$to a_5.

4.2. Support vector regression (SVR) model

4.2.1. Theoretical background

SVR is the extension of SVM and it has been used successfully for the purpose of regression on many engineering problems. The basic goal is to accurately fit a regression function, y = f (x) in a ε-SVR model so as to accurately predict the targets $\{y_i\}$ corresponding to a set of input samples, $\{x_i\}$, With the given training data set as D= $\{(x_1, y_1), (x_2, y_2), \ldots, (x_N, y_N)\}$, where xi ϵ R_N is a vector of input variables and yi ϵ R_N is the corresponding scalar output (target) value. For the non-linear problems of the real world where the input data cannot be correlated to the required output linearly, the

Table 3
Details of the parameters under consideration of the splice specimens tested in this study.

Beam ID	Width of the beam w (mm)	Bar diameter d_b (mm)	Compressive Strength f_{ck} (MPa)	Cover		Splice length l_s (mm)	Splice strength f_s (MPa)
				C_{min} (mm)	C_{max} (mm)		
A	150	12	45.6	20	31	120	377.99
B	200	12	48.2	36	40	120	450
C	150	20	46.8	15	20	200	198.94
D	230	20	47.6	35	40	200	276.56

Table 4
Ranges of the input and output parameters considered in the formulation of models.

Parameters	d_b (mm)	C_{min}/d_b	l_s/d_b	$f_c^{'}$ (MPa)	Stress in steel (MPa)
Range	10–60	0.50–3.33	9.21–80	16.4–108.5	193–678

following linear model can be constructed in the high-dimensional feature space using a nonlinear mapping function $g_i(x)$ as given in Eq. (9).

$$f(x,\omega) = \sum_{i=1}^{n} \omega_i g_i(x) + b \tag{9}$$

where $g_i(x)$ is the function termed feature and $\omega_i.g_i(x)$ is the dot product in the feature space F and b is the bias. It works on the principle of structural risk minimization [44]. The coefficients can be estimated by minimizing the risk function which is stated as:

$$R(C) = C\frac{1}{l}\sum_{i=1}^{l} L_c(y_i, f(x_i,\omega)) + \frac{1}{2}\|\omega\|^2 \tag{10}$$

The risk function (Eq. (10)) is the summation of two terms namely, the empirical error term

$C\frac{1}{l}\sum_{i=1}^{l} L_c(y_i, f(x_i,\omega))$ and the flatness or smoothness of the function $\frac{1}{2}\|\omega\|^2$. The empirical error term consists of a function called ε-insensitive loss function $L_c(y_i, f(x_i, \omega))$ and a factor C.

Where,

$L_c(y_i, f(x_i, \omega)$ =

$$\begin{cases} |y - f(\omega)| - \varepsilon, for |y - f(x,\omega)| \le \varepsilon \\ 0, for |y - f(x,\omega)| > \varepsilon \end{cases} \tag{11}$$

where C factor is the measure of the extent of the trade-off between the empirical error and the model flatness. In order to account for the errors exceeding the limit ε, positive constants called as slack variables ξ,ξ^* are introduced. The slack variables in turn covert the SVR problem into a dual optimization problem whose objective function is

Minimization of

$$z(\omega, b, \xi, \xi^*) = \frac{1}{2}\|\omega\|^2 + C\sum_{i=1}^{l}(\xi_i + \xi_i^*) \tag{12}$$

Subjected to constraint equations

$$y_i - f(x_i,\omega) \le \varepsilon + \xi_i \tag{12a}$$

$$f(x_i,\omega) - y_i \le \varepsilon + \xi_i^* \tag{12b}$$

$$\xi_i, \xi_i^* \ge 0 \tag{12c}$$

The well-known Lagrangian multiplier strategy was adopted to solve the convex optimization problem. The transformed equation with the multipliers is as follows.

$$f(x, \alpha_i, \alpha_i^*) = \sum_{i=1}^{N}(\alpha_i - \alpha_i^*)(g(x_i).g(x_j)) + b \tag{13}$$

where α_i and α_i^* are the Lagrangian multipliers. The input vector x_i are called as the support vectors provided their corresponding coefficients $(\alpha_i - \alpha_i^*) \neq 0$. These vectors are the representative of the entire support vector function as they contain most of the information of the training data set. To overcome the contradiction between the high dimensional featured space and the complexity in computation, proper kernel function should be defined [44]. Any function which is symmetric, positive and semi-definite (Mercer's condition) qualifies to be a kernel function [45]. Among the generally used kernel functions, the Gaussian radial basis function (RBF) is the most common one. The description of the function is as follows [46–47].

$$K(x_i, x_j) = (g(x_i)g(x_j)) = \exp\left(-\frac{1}{2\sigma^2}\|x_i - x_j\|^2\right) = \exp\left(-\gamma\|x_i - x_j\|^2\right) \tag{14}$$

where, $i,j = 1 \cdots .. N$.

where σ is the width of the RBF and γ equals to $1/(2.\sigma^2)$

Hence, with the aid of the kernel function, all the computations regarding g can be performed in an explicit manner in the input space itself without actually bothering the featured space. The basic equation describing the modeling of the data is as follows:

$$f(x, \alpha_i, \alpha_i^*) = \sum_{i=1}^{N}(\alpha_i - \alpha_i^*)(K(x_i, x_j) + b \tag{15}$$

The parameter b can be estimated by applying Karush–Kuhn–Tucker (KKT) conditions as follows

$$b = -\frac{1}{2}\sum_{i=1}^{N}(\alpha_i^* - \alpha_i)g[(x_m, x_i) + K(x_n, x_i)] \tag{16}$$

where x_m, x_n are the support vectors.

4.2.2. Model formulation

For the purpose of model formulation, the significant parameters identified earlier were used as input parameters i.e. d_b (diameter of the bar), l_s (development length), (compressive strength), C_{max} and C_{min} (cover to the concrete maximum and minimum). Also, the same randomly generated training data set and the test set as used for the NMR model was used for the training and testing of the SVR model. The kernel chosen for the modeling SVR was RBF which is described by the Eq. (14). The RBF kernel was preferred over other kernels due to its relatively better general performance and dependency on only one parameter γ. However, for the good generalization performance of SVR, apart from kernel selection, proper selection of the parameters is quintessential. It has been observed that the grid search methodology if used in conjunction with a 10-fold cross-validation procedure yields the optimum value of the parameters on the training set. It not only minimizes the average absolute relative error (AARE) but also converges the correlation coefficient (R) value to 1.

4.3. Artificial neural network model

4.3.1. Theoretical background

ANN is an attempt to simulate the biological functioning of the human brain. It is based on realizing a mathematical relationship between the input and output parameters through a process of learning. The relationship between the input parameter and the output ones is

$$Y_k = F(I) = F(b + \sum_{k=1}^{N} w_k x_k) \tag{17}$$

The learning or training can be performed by a network of artificial neurons often called as perceptrons. These terms are often interchangeably used in the world of machine learning. These perceptrons are mathematical functions/transfer functions that simulate the biological neuron function. These functions can be linear, sigmoidal, step and sometimes used in a combination of two. Among the various choices, the sigmoidal function is the most popular among all. The function generally appears to be as

$$\Psi(x) = \frac{1}{(1 + e^{-x})} \tag{18}$$

These are generally arranged in layers of one or more than one and hence called as Multilayer perceptron. This network is generally used in the learning process and is very popular among the engineering community [48,49]. By the virtue of the utilization of layers inside the network, they are classified as the input layer, hidden layer and the output layer. As the name suggests the input layer perceptron receives information of the different variables from the external environment. The perceptron may receive single or multiple inputs depending upon the architecture of the network.

This input information is used by the perceptron in the hidden layer for the calculation of the weighted sum. Latter through a transfer function these values are transferred to the output layer for the calculation of error.

The back-propagation algorithm has been commonly used to minimize the error of the network system. The algorithm works on the principle of error minimization by sending the error from the output layer directly as an input in the input layer. The process is multi-iterative in nature, each time error is considered as input, weights are adjusted and it continues till the error converges to the minimum. A simple illustration of the optimization algorithm is shown in Fig. 2.

4.3.2. ANN model formulation

As a typical AI methodology, the network selected (MLP) was first trained and then tested. The same randomized data set as previously utilized for developing NMR and SVR was chosen for the learning and testing of the ANN model. The underlining fact beneath this idea was to ascertain a fair comparison among the three models. The back-propagation algorithm was used with a single hidden layer for the purpose of training. The network weights were adjusted by applying the Levenberg–Marquardt algorithm (LMA) [50,51] on the training data set rather than the traditional BP algorithm. Among all other algorithms, LMA is very popular among the researchers because of its faster convergence although it consumes larger memory space. With regard to the transfer function, the non-linear sigmoidal function was utilized inside the hidden layer while the linear function was used for the output layer.

Depending upon the input parameters and the output parameters, the feed-forward network has five input neurons while one output neuron. After multiple iterations were performed on the network, the number of neurons was eleven in the hidden layer. The trained network obtained is as shown in Fig. 3.

5. Performance evaluation of the models

Statistical analysis was performed to evaluate the efficacy of the different models which included existing correlations as well the three proposed ones with the help of well-known statistical parameters: AARE, RMSE, Q2L100, Q2EXT, and MRE which are defined as follows:

(a) AARE: Absolute average relative error

$$= \frac{1}{N}\sum_{i=1}^{N}\left|\left[\frac{y_{pre}-y_{exp}}{y_{exp}}\right]\right| \tag{19}$$

(b) RMSE: Root mean square

$$= \sqrt{\frac{\sum_{i=1}^{N}\left[(y_{exp}-y_{pred})/y_{pred}\right]^2}{n}} \tag{20}$$

(c) MRE: Mean relative error

$$= \frac{1}{N}\sum_{i=1}^{N}\left|\left[\frac{y_{exp}-y_{pre}}{y_{pre}}\right]\right| \tag{21}$$

(d) Q^2_{LOO}: It is a measure of the internal capability of prediction of the SVR model and often assessed as leave one out cross-validation on the training data [52].

$$= \frac{\sum_{i=1}^{n_{training}}\left(y_{exp}-y_{pre}\right)^2}{\sum_{i=1}^{n_{training}}\left(y_{exp}-y_{pre}^{mean}\right)^2} \tag{22}$$

(e) Q^2_{ext}: It is the measure of the external capability of the prediction of the SVR model and often assessed as leave one out on the test data [52].

$$= \frac{\sum_{i=1}^{n_{test}}\left(y_{exp}-y_{pre}\right)^2}{\sum_{i=1}^{n_{test}}\left(y_{exp}-y_{tr}^{mean}\right)^2} \tag{23}$$

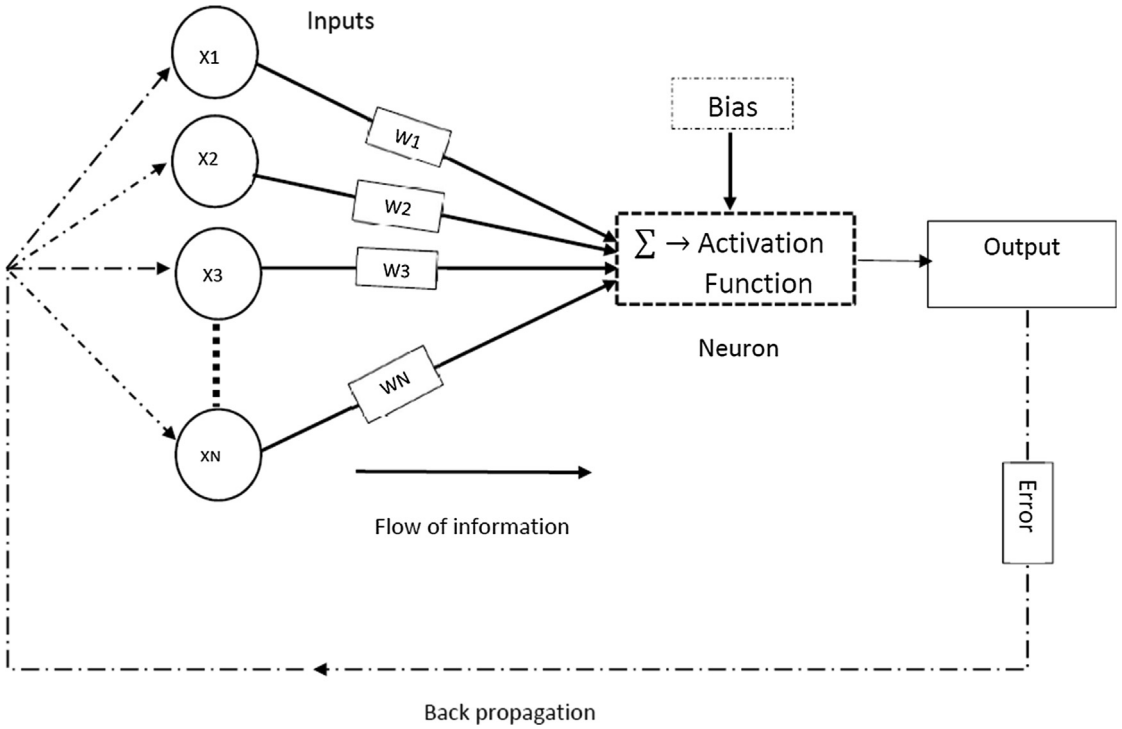

Fig. 2. Optimization of the neural network through feed forward back propagation method.

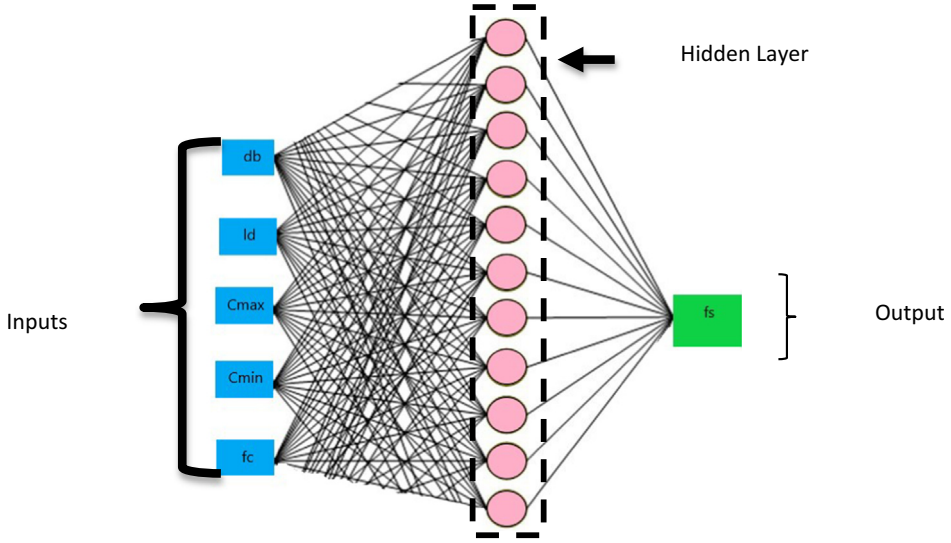

Fig. 3. Detailed description of the formulated ANN model.

6. Results and discussions

6.1. Analysis of the NMR model

The regression was performed on the training data set using d_b (diameter of the bar), l_s (development length), $f_c^{'}$ (compressive strength), C_{max} and C_{min} (cover to the concrete maximum and minimum) as the independent parameters and f_s (stress in steel) as the dependent parameter. The following NMR model equation is obtained

$$fs = 35.45 * (d_b)^{-1}.(l_s)^{0.5}.\left(f_c^{'}\right)^{0.23}.(C_{min}.C_{max})^{0.17} \quad (24)$$

Fig. 4 shows that the prediction from the obtained model for both the training and the test values are well within the line of the experimental data. The observed AARE (%) for the training and test data are obtained to be 9.5% and 9.2% respectively. Also, the values of MRE and RSME for the training data set are 0.094 and 0.121 while for the test data set they are observed to be 0.088 and 0.097, respectively, which shows that in the domain of test data the model shows better generalization performance.

6.2. Analysis of the SVR based model

To optimize the model parameters C and ε and the RBF kernel parameter γ, gridsearch methodology in conjunction with 10 folds-cross validation was performed. The model parameters C and ε and the kernel parameter γ were varied in the corresponding ranges of (2^2-2^{15}), (2^{-10}-2^5) and (2^{-10}-2^4) respectively. Their optimized values are listed in Table 5. The optimized model was used to plot the training course curve and test course curve as shown in Fig. 5. It is evident that the predicted values are close to the experimental ones. The performance parameters AARE, RMSE and MRE for the training data are found to be 8.2, 0.10, and 0.083, respectively while for the test data these values are 8.3, 0.096, and 0.076, respectively, which suggested that the performance of the SVR based model is generalized.

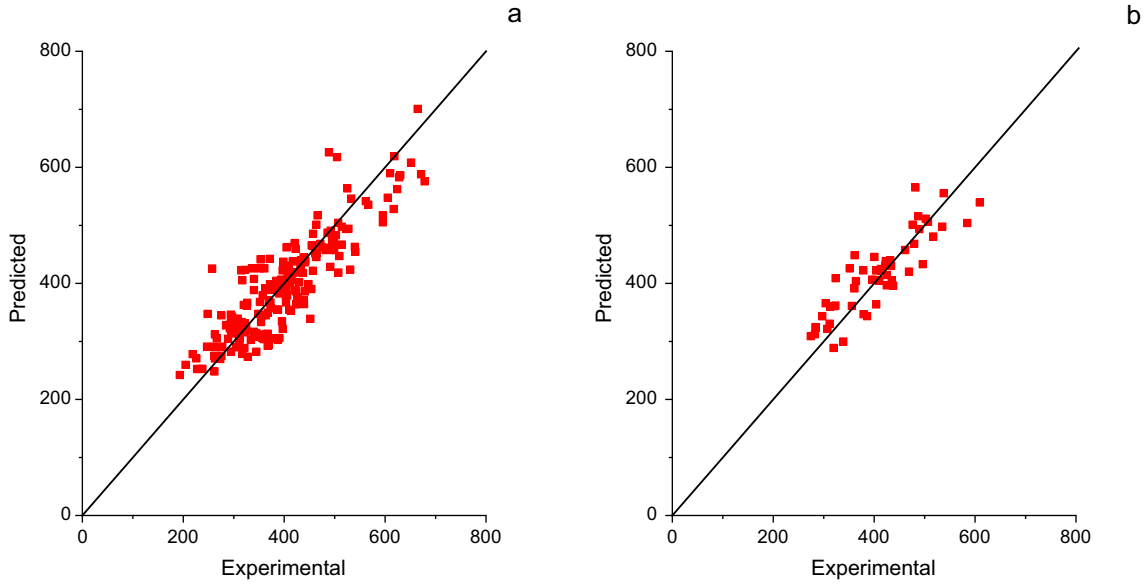

Fig. 4. Comparison of the predicted experimental (a) training and (b) test course curve for NMR.

Table 5
Optimal parameters for the SVR based model for the stress in steel in splice beam specimens.

Model	C	γ	ε	Kernel type	Type of loss function	Number of support vectors	Number of training points
Splice strength	4096	1	2	RBF	εinsensitive	89	207

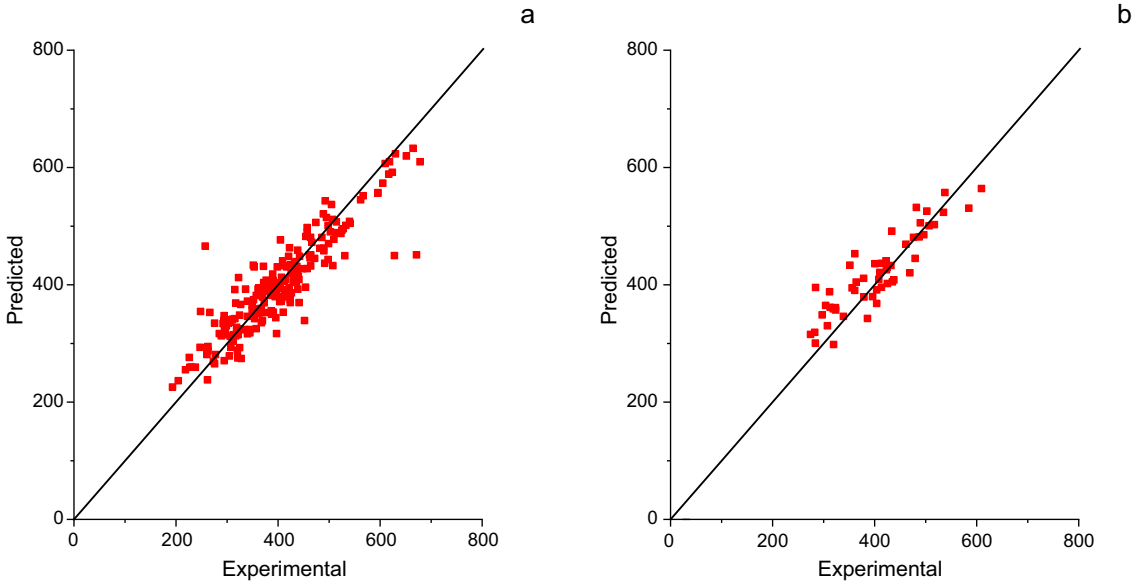

Fig. 5. Comparison of the predicted and experimental (a) training and (b) test course curve for SVR.

6.3. Analysis of the ANN model

The weights of the network were optimized during the training of the network. The training and test course curves are plotted in Fig. 6. They suggest close prediction of the experimental data of the splice strength by the ANN model. The values of the statistical parameters of the ANN model i.e. AARE, RMSE and MRE values for the training data set are observed to be 7.0, 0.095, and 0.066, respectively. The corresponding values for the test data are 8.8, 0.10, and 0.080, respectively, which shows that the ANN model gives a generalized performance. One can infer the fact that the prediction capability of the model is consistent.

6.4. Comparison of the different developed models with the other correlations available in the literature

Fig. 7 illustrates the comparison of the ratios of predicted to observed (RPO) splice strength of the unconfined beam specimens by the three formulated models of the existing study with those from literature. A preliminary look shows that in comparison to

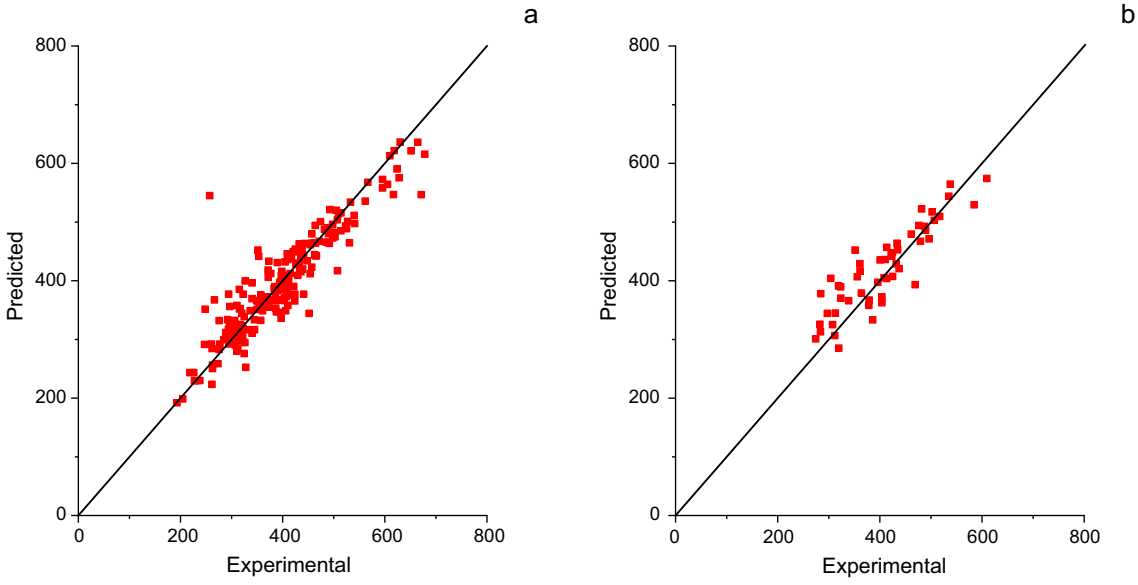

Fig. 6. Comparison of the predicted and experimental (a) training and (b) test course curves for the ANN model.

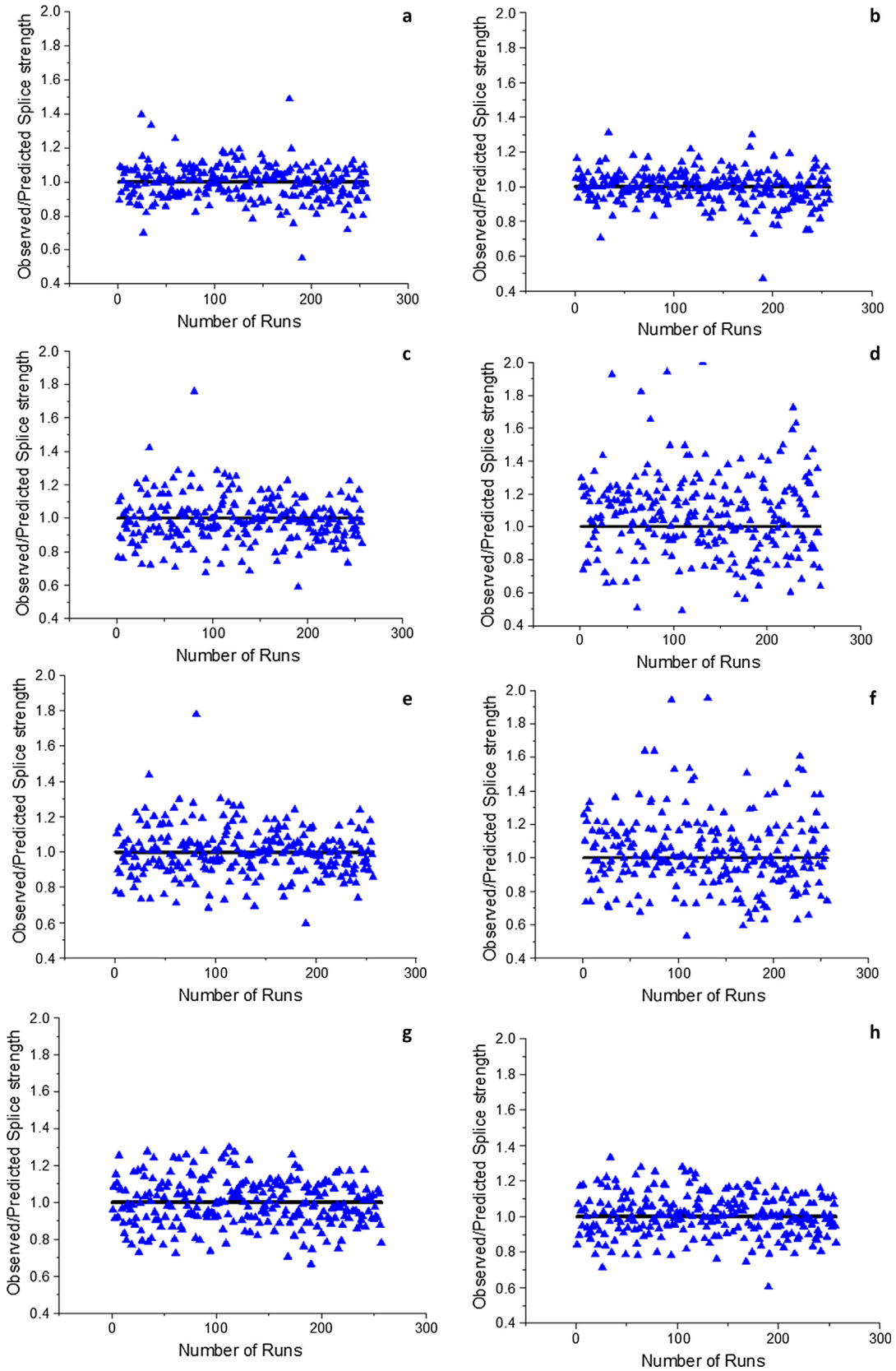

Fig. 7. Comparison of the ratio of the observed to predicted splice strength of the various models (a) SVR (b) ANN (c) ACI 408-R (d) OJB (e) Zuo and Darwin (f) Esfahni and Ranjan (g) FIB model code 2010 and (h) NLR.

the other existing empirical correlations [10,14,15,13,16] the (RPO) of the splice strength by the NMR model lies close to the unity line. Also, when the statistical parameters AARE, RSME, MRE, Q_{loo} of the NMR model are compared with the empirical correlations as shown in Table 6, the NMR exhibits the minimum values of 9.2, 0.1166, 0.0914 and 0.2265, respectively, which shows that the

Table 6
Comparison of statistical performance parameters for various models.

Model evaluation parameters	AARE (%)	RMSE	MRE	Q_{LOO}	Q_{EXT}
SVR based model	8.221	0.1047	0.0790	0.1862	0.2288
ANN	7.346	0.0961	0.0689	0.1598	0.2497
NMR	9.291	0.1166	0.0914	0.2265	0.2428
Orangan Jirsa [10]	18.571	0.2529	0.1944	1.135	1.764
Zuo & Darwin [14]	10.543	0.1381	0.1022	0.3547	0.3006
ACI 408 R [15]	10.657	0.1365	0.1014	0.3612	0.3202
Esfani & Ranjan [13]	15.872	0.2656	0.1698	0.9406	1.2784
Model Code 2010 [16]	10.538	0.1254	0.1018	0.2977	0.3184

NMR model is better among all existing empirical models in predicting the splice strength.

However when the RPO splice strength values predicted by the machine learning models (ANN and SVR) are compared with the typical empirical NMR model, it has been observed that the RPO of the splice strength of ANN and SVR are closer to the unity value as compared to NMR. This shows that the AI models possess less susceptibility for over or under-prediction of the splice strength. Furthermore, the parameters namely, AARE, RMSE, and MRE give lesser values for the AI models as compared to empirical models from literature and the NMR model as shown in Table 6. This shows that the prediction capability of the AI models is superior to that of the empirical models from literature and the NMR model.

When comparing among the two AI models i.e. SVR and ANN, the ANN shows a relatively better fit as shown in Fig. 7 (a-b). The statement can be statistically supported by the fact that the AARE value of ANN is 7.34% while it is 8.22% for the SVR model. Other than the AARE, the ANN model exhibits lesser values of the other statistical parameters namely, RMSE and MRE as shown in Table 6, which further confirms better prediction by the ANN model. However, even though the ANN is giving slightly superior results in this case than its SVR counterpart but the small number of parameters to be optimized, the existence of a unique solution and less computational efforts required for the development of the SVR model gives an edge to this technique over the ANN. Also, the SVR is capable of providing a sparse solution whereas the ANN cannot. This means that while the SVR model utilizes only 89 data points (support vectors) to give the model as listed in Table 5, the ANN model needs 259 data points for the optimization.

6.5. Probable impact of these new prediction tools for the bond research community

This work is of great interest to the researchers in the field of bond as the two techniques namely, ANN and SVR are Machine Learning (ML) methods. Machine learning is a data analytics technique that imparts computers the capability to learn from experience. This is what humans and animals do naturally. ML algorithms use computational methods to "learn" information directly from data without relying on a predetermined equation as a model. The algorithms progressively improve their performance as the amount of data available for learning increases. The detection of natural patterns in the data generates insight and helps the engineer to make better decisions and predictions. ML techniques are broadly divided into two groups namely, supervised learning and unsupervised learning. Supervised learning uses a known set of input data and known responses to the data and trains a model to generate reasonable predictions for the response to new data. ANN and SVR techniques belong to this category. While unsupervised learning is a type of ML algorithm that draws inferences from datasets consisting of input data only without labeled responses. There are several techniques under both categories of ML. However, in both types, the machine learns with more and more data. There is tremendous scope in this field for the researchers in the civil engineering community in general and the bond community in particular to develop more robust and accurate models can be made with additional data. As a small beginning, this work has used only two supervised ML techniques with a limited amount of data and both the models have outperformed the existing empirical models. With more data, still better ML models can be made using these two algorithms. Other ML techniques are also open for exploration to develop more efficient and accurate models to solve the complex problem of the prediction of lap splice without actually going into the mechanics.

7. Conclusions

The three models that have been developed in this study for the assessment of the splice strength of beam specimens have been assessed and are compared to the existing empirical models for their performances. Among all existing empirical correlations, the non-linear multi regression (NMR) model proved to be the most accurate in predicting the splice strength of the beam specimens. The model bears simple exponents of the most significant parameters affecting the splice strength. However, the optimized SVR model which has been developed for the first time in the literature to predict the splice strength of the beam specimens shows superior prediction ability in comparison to all other existing correlations including the NMR model. The SVR model also illustrates lesser susceptibility to over-fitting or under-fitting for the splice strength of beams which is otherwise absent in the empirical models. The ANN-based model was found to give a slightly better prediction of splice strength than the SVR model but at the cost of higher computational effort and the risk of it getting stuck in local minima during optimization. On the other hand, the SVR model presented an efficient, robust and less parameter model with faster convergence and sparse solution. Thus, it can be concluded that the SVR technique can be successfully applied to the complex problem of predicting the splice strength of the beam specimens.

Credit authorship contribution statement

Mohammad Suhaib Ahmad: Conceptualization, methodology, validation, writing - original draft, formal analysis and investigation. **Sayed Mohammad Adnan:** Software. **Sadaf Zaidi:** Supervision and resources. **Pradeep Bhargava:** Project administration and resources.

Declaration of Competing Interest

The authors declare that they have no known competing financial interests or personal relationships that could have appeared to influence the work reported in this paper.

References

[1] A. Azizinamini, M. Chisala, S.K. Ghosh, Tension development length of reinforcing bars embedded in high-strength concrete, Eng. Struct. 17 (7) (1995) 512–522.
[2] P.G. Gambarova, G.P. Rosati, B. Zasso, Steel-to-concrete bond after concrete splitting: test results, Mater. Struct. 22 (1) (1989) 22–35.
[3] F. De Larrard, I. Shaller, J. Fuchs, Effect of the bar diameter on the bond strength of passive reinforcement in high-performance concrete, Mater. J. 90 (4) (1993) 333–339.
[4] D. Darwin, E. Graham, Effect of deformation height and spacing on bond strength of reinforcing bars, ACI Mater. J. 90 (1993) 646–657.
[5] J. Zuo, D. Darwin, Splice strength of conventional and high relative rib area bars in normal and high-strength concrete, ACI Struct. J. 97 (2000) 630–641.
[6] J. Cairns, K. Jones, Influence of rib geometry on strength of lapped joints: an experimental and analytical study, Mag. Concr. Res. 47 (172) (1995) 253–262.
[7] D. Darwin, M. Tholen, E.K. Idun, J. Zuo, Splice strength of high relative rib area reinforcing bars, ACI Struct. J. 93 (1) (1996) 95–107.
[8] J. Cairns, C. Goodchild, Effect of reduced concrete cover on strength of lapped joints, Proc. Instit. Civil Eng.-Struct. Build. 169 (1) (2016) 34–45.
[9] R. Eligehausen, E.P. Popov, V.V. Bertero, Local bond stress-slip relationships of deformed bars under generalized excitations, in: Earthquake Engineering Research Center Report, University of California, Berkeley, 1982, pp. 82–83.
[10] C.O. Orangun, J.O. Jirsa, J.E. Breen, Reevaluation of test data on development length and splices, J. Am. Concr. Inst. 74 (3) (1977) 114–122.
[11] R. Tepfers: A Theory of Bond Applied to Overlapped Tensile Reinforcement Splices for Deformed Bars. Publ 73:2. Division of Concrete Structures, Chalmers University of Technology, Göteborg, May 1973, p. 328. Doktorsavhandling. http://document.chalmers.se/doc/697703874, 1973.
[12] M.R. Esfahani, B.V. Rangan, Local bond strength of reinforcing bars in normal strength and high-strength concrete (HSC), ACI Struct. J. 95 (2) (1998) 96–106.
[13] M.R. Esfahani, B.V. Rangan, Bond between normal strength and high-strength concrete (HSC) and reinforcing bars in splices in beams, ACI Struct. J. 95 (3) (1998) 272–280.
[14] J. Zuo, D. Darwin, Bond Strength Of High Relative Rib Area Reinforcing Bars, 1998. SM Report No. 46, University of Kansas Center for Research, Lawrence, Kans 350 pp.
[15] ACI 408 Committee, Bond and Development of Straight Reinforcing Bars in Tension (ACI 408R-03), American Concrete Institute, Detroit, Michigan, US, 2003.
[16] CEB-FIP Model Code 2010, Fib Model Code for Concrete Structures 2010, Ernst & Sohn, Wiley, Berlin, Germany, 2013.
[17] A. Behnood, K.P. Verian, M. Modiri Gharehveran, Evaluation of the splitting tensile strength in plain and steel fiber-reinforced concrete based on the compressive strength, Constr. Build. Mater. 98 (2015) 519–529.
[18] M.M. Alshihri, A.M. Azmy, M.S. El-Bisy, Neural networks for predicting compressive strength of structural light weight concrete, Constr. Build. Mater. 23 (6) (2009) 2214–2219.
[19] Z. Dahou, Z. Mehdi Sbartaï, A. Castel, F. Ghomari, Artificial neural network model for steel–concrete bond prediction, Eng. Struct. 31 (8) (2009) 1724–1733.
[20] E.M. Golafshani, A. Rahai, M.H. Sebt, H. Akbarpour, Prediction of bond strength of spliced steel bars in concrete using artificial neural network and fuzzy logic, Constr. Build. Mater. 36 (2012) 411–418.
[21] P. Yuvaraj, A. Ramachandra Murthy, N.R. Iyer, S.K. Sekar, P. Samui, Support vector regression based models to predict fracture characteristics of high strength and ultra high strength concrete beams, Eng. Fract. Mech. 98 (2013) 29–43.
[22] H. Abbas, Y.A. Al-Salloum, H.M. Elsanadedy, T.H. Almusallam, ANN models for prediction of residual strength of HSC after exposure to elevated temperature, Fire Saf. J. 106 (2019) 13–28.
[23] H. Erdem, Predicting the moment capacity of RC beams exposed to fire using ANNs, Constr. Build. Mater. 101 (2015) 30–38.
[24] Y. Yu, W. Li, J. Li, T.N. Nguyen, A novel optimised self-learning method for compressive strength prediction of high performance concrete, Constr. Build. Mater. 184 (2018) 229–247.
[25] P. Samui, Support vector machine applied to settlement of shallow foundations on cohesionless soils, Comput. Geotech. 35 (3) (2008) 419–427.
[26] IS 8112-1989: (re-affermed in 2000), Specification for 43grade ordinary portland cement, Bureau of Indian Standards, New Delhi, India.
[27] IS 383-1970: Specification for course aggregate and fine aggregate from natural source for concrete,Bureau of Indian Standards, New Delhi, India.
[28] R. Tepfers, Bond stress along lapped reinforcing bars, Mag. Concr. Res. 32 (112) (1980) 135–142.
[29] J. Chinn, P.M. Ferguson, J.N. Thompson, Lapped splices in reinforced concrete beams, ACI J. Proceed. 52 (2) (1955) 201–213.
[30] S.J. Chamberlin, Spacing of reinforcement in beams, ACI J. Proc. 53 (7) (1956) 113–134.
[31] S.J. Chamberlin, Spacing of spliced bars in beams, ACI J. Proc. 54 (2) (1958) 689–697.
[32] P.M. Ferguson, J.E. Breen, Lapped splices for high strength reinforcing bars, ACI J. Proceed. 62 (9) (1965) 1063–1078.
[33] M.A. Thompson, J.O. Jirsa, J.E. Breen, D.F. Meinheit, Behavior of multiple lap splices in wide sections, ACI J. Proceed. 76 (2) (1979) 227–248.
[34] P.M. Ferguson, J.N. Thompson, Development length for large high strength reinforcing bars, ACI J. Proceed. 62 (1) (1965) 71–93.
[35] R. Mathey, D. Watstein, Investigation of bond in beam and pull-out specimens with high-yield-strength deformed bars, ACI J. Proc. 58 (9) (1961) 1071–1090.
[36] C.J. Hester, S. Salamizavaregh, D. Darwin, S.L. McCabe, Bond of Epoxy-Coated Reinforcement: Splices, ACI Struct. J. 90 (1) (1993) 89–102.
[37] O.C. Choi, H. Hadje-Ghaffari, D. Darwin, S.L. McCabe, Bond of epoxy-coated reinforcement: bar parameters, ACI Mater. J. 88 (2) (1991) 207–217.
[38] A.J. Zekany, S. Neumann, J.O. Jirsa, J.E. Breen, The Influence of Shear on Lapped Splices in Reinforced Concrete, Research Report 242-2, Center for Transportation Research, Bureau of Engineering Research, University of Texas at Austin, Tex, 1981.
[39] T. Rezansoff, A. Akanni, B. Sparling, Tensile lap splices under static loading: a review of the proposed ACI 318 code provisions, ACI Struct. J. 90 (4) (1993) 374–384.
[40] D. Darwin, J. Zuo, M. Tholen, E.K. Idun, Development length criteria for conventional and high relative rib area reinforcing bars, ACI Struct. J. 93 (3) (1996) 347–359.
[41] H. Marzouk, H. Marzouk, Bond behaviour of high strength concrete, Mag. Concr. Res. 545 (2004).
[42] A. Azizinamini, R. Pavel, E. Hatfield, S.K. Ghosh, Behavior of spliced reinforcing bars embedded in high strength concrete, ACI Struct. J. 96 (5) (1999) 826–835.
[43] B.S. Hamad, M.S. Itani, Bond, Strength of reinforcement in high-performance concrete: the role of silica fume, casing position, and superplasticizer dosage, ACI Mater. J. 95 (5) (1998) 499–511.
[44] R.G. Brereton, G.R. Lloyd, Support vector machines for classification and regression, Analyst 135 (2) (2010) 230–267.
[45] Y. Pan, J. Jiang, R. Wang, H. Cao, Y. Cui, A novel QSPR model for prediction of lower flammability limits of organic compounds based on support vector machine, J. Hazard. Mater. 168 (2) (2009) 962–969.
[46] A.J. Smola, B. Schölkopf, A tutorial on support vector regression, Statist. Comp. 14 (3) (2004) 199–222.
[47] V. Vapnik, S.E. Golowich, A. Smola, Support vector method for function approximation, regression estimation and signal processing, in: Proceedings of the 9th International Conference on Neural Information Processing Systems, MIT Press, Denver, Colorado, 1996, pp. 281–287.
[48] N. Caglar, Neural network based approach for determining the shear strength of circular reinforced concrete columns, Constr. Build. Mater. 23 (10) (2009) 3225–3232.
[49] P. Cachim, Using artificial neural networks for calculation of temperatures in timber under fire loading, Constr. Build. Mater. 25 (11) (2011) 4175–4180.
[50] D.W. Marquardt, An algorithm for least-squares estimation of nonlinear parameters, J. Soc. Ind. Appl. Math. 11 (2) (1963) 431–441.
[51] A. Suratgar, M.B. Tavakoli, A. Hoseinabadi, Modified Levenberg-Marquardt Method for Neural Networks Training, Proceedings – Wec 05: Fourth World Enformatika Conference 6, 2005.
[52] P. Gramatica, Principles of QSAR models validation: internal and external, QSAR Comb. Sci. 26 (5) (2007) 694–701.